ELSEVIER

Journal of Molecular Catalysis A: Chemical 126 (1997) 61–72

JOURNAL OF MOLECULAR CATALYSIS A: CHEMICAL

Ab initio calculations on the mechanisms of hydrocarbon conversion in zeolites: Skeletal isomerisation and olefin chemisorption

A.M. Rigby *, M.V. Frash

Shell Research and Technology Centre, Shell International Oil Products B.V., P.O. Box 38000, 1030 BN Amsterdam, The Netherlands

Abstract

Quantum chemical calculations on zeolite-catalysed hydrocarbon conversion mechanisms have been carried out. The one-step skeletal isomerisation (methyl shift) and the olefin chemisorption reactions have been considered. The results obtained indicate that the product distribution of both reactions are determined by the activation energies rather than by the reaction heats. The shift of an existing branch is calculated to be significantly (by about 10 kcal/mol) easier than branch formation in *n*-alkanes in agreement with the experimental data. Only a small difference is found between *n*-butane and *n*-pentane isomerisation, which contrasts with experiment and suggests that at least one of these reactions does not proceed via a one-step methyl shift. Calculations show also that alkyl groups larger than methyl may be shifted. © 1997 Elsevier Science B.V.

Keywords: Hydrocarbon conversion; Olefin chemisorption; Skeletal isomerisation; Transition states; Zeolite catalysts

1. Introduction

Solid acid catalysts based on zeolites play an important role in the hydrocarbon conversion processes in a modern refinery [1,2]. Amongst other applications they are used in the isomerisation of paraffins and the FCC and hydrocracking processes. An understanding of the conversion mechanisms taking place on the active Brønsted acid sites of the zeolites would be valuable in improving existing catalysts and developing new ones, especially if the influence on the catalytic behaviour of changes in the zeolite (such as the acid strength) or differences between hydrocarbons could be included.

However, many elementary steps of the hydrocarbon conversion are not accessible for direct experimental studies since there are usually several reactions occurring simultaneously and the influence of adsorption and diffusion of the reactants and products is difficult to describe. Recently quantum mechanical calculations have begun to be used to gain insight into the mechanisms. Based on quantum–chemical results [3] together with IR data, Kazansky has shown [4] that the relatively stable intermediates in the reactions are not carbocations but alkoxide species in which the hydrocarbon is covalently bound to the acid site, and showed for olefin chemisorption that the carbocation is the transi-

* Corresponding author. Tel.: +31-20-6309111; fax: +31-20-6308025.

PII S1381-1169(97)00095-2

tion state. Detailed calculations on the D–H exchange between the acid site and methane [5,6] which can be experimentally studied in isolation, showed that the approach could quantitatively describe the differences in reactivity between zeolites.

Extending this work, the commercially important reaction steps, such as methyl shift and β-scission have been investigated in Ref. [7]. However in these calculations planar symmetry was imposed on the systems and the effect of these on the quality of the results is not known. These symmetry constraints also restrict the examples that can be considered in an investigation of the differences between hydrocarbons.

This paper will describe calculations for a much wider set of hydrocarbons. Two reaction steps will be considered: the internal methyl shift reaction and the olefin chemisorption. The internal methyl shift is the simplest possible pathway for the skeletal isomerisation of hydrocarbons. The skeletal isomerisation is an important commercial process in its own right, and it plays an important role in the product distribution of other commercial reactions including cracking and alkylation [1]. Due to its importance, skeletal isomerisation of hydrocarbons on solid acid catalysts was a subject of extensive experimental investigations (e.g., Refs. [8–24]). However, previous quantum–chemical calculations [7] considered only two examples of this reaction. The olefin chemisorption is an elementary step in many processes (especially those involving a hydrogenation function) and is responsible for the double bond shift in olefins. The olefin chemisorption has been investigated previously by means of quantum–chemical methods [3,7,25–27] but the effect of different olefins was not considered in details.

The investigations of the conversion transition states [7] indicated that the transition states for most of the conversion reactions are ionic. Olefin chemisorption is a partial exception being less ionic than other reactions. This is shown by the sensitivity to the acid strength of the acid site. To investigate whether these conclusions also hold in the absence of symmetry constraints the acidity variation of the methyl shift step was compared with calculations of the olefin chemisorption transition state. It is also interesting to see how the effect of methyl substitution and the strength of acid site can both be related to the ionicity of the reaction.

2. Models and computational details

All the computations were performed with the GAMESS-UK ab initio program [28], based on the Hartree-Fock (HF) and second order Møller-Plesset (MP2) approximations [29]. The Brønsted acid sites of zeolites were modelled by the $H_3Si–(OH)–AlH_2–O–SiH_3$ cluster (see Fig. 1a). The geometries of the structures investigated were optimised at the HF level with the standard 3-21G basis set. During the optimisation, the aluminium, both silicon, and both oxygen atoms of the cluster were kept in one plane, to suppress soft modes for the distortion of the cluster which have little influence on the energy but cause optimisation difficulties and are not present in real zeolites. No other geometry constraints were applied. Transition states were

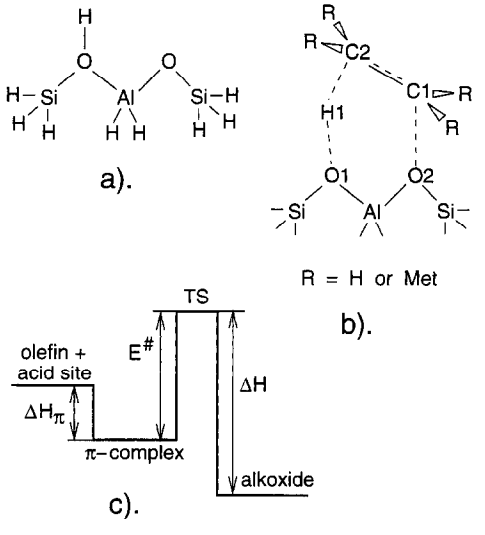

Fig. 1. (a) Model Brönsted acid site cluster. (b) Scheme of the olefin chemisorption transition state. (c) Energy diagram for olefin chemisorption.

tested by distorting the structure a little in the direction of the negative eigenvector and then optimising them to find the initial and final states involved.

Reaction heats and activation energies have been calculated at the MP2(FC)/6-31G*//3-21G level. It should be noted that there are two slightly different versions of the 6-31G basis sets for silicon [30,31] and the GAMESS-UK default [30] was used in the present calculations. No corrections for zero-point energies and for basis set superposition errors were taken into account. Atomic charges have been calculated according to the DMA scheme [32] at the HF/3-21G level.

A given surface alkoxide can have several isomers and many conformers. Total energy differences between isomers can be significant (up to 3–5 kcal/mol) and therefore all the isomers of alkoxides involved in the reactions have been calculated. However, the range of energy differences between conformers has been found to be small, for instance conformers of different propyl alkoxides differ by less than 1 kcal/mol both at the HF/3-21G and MP2/6-31G*//3-21G levels. Therefore, the conformers were not considered further.

3. Results and discussion

3.1. Olefin chemisorption

The olefin chemisorption reaction or its reverse is responsible for olefin release during cracking (both FCC and hydrocracking), double-bond shift in olefins (e.g., but-1-ene to but-2-ene) and interconversion between surface alkoxides with the same carbon skeletons. Differences between olefins and between the positions of the adsorption can cause different reaction products. In the carbenium ion model of the conversion reactions often used, these differences are predicted on the basis of an energy ordering of the ionic intermediates (tertiary > secondary > primary in stability). However, previous calculations have shown that the actual intermediates are alkoxides [3,4] and do not have a large energy ordering [7]. Therefore, any difference between the hydrocarbon conversion reactions in zeolite catalysts must be described by differences in the activation energies.

In the transition states the hydrocarbon portion is found to be positively charged and the differences in activation energies are due to stabilisation by alkyl groups bound to the charged carbon atoms. The conversion transition states with the exception of olefin chemisorption and D/H exchange are approximately equally ionic [7]. D/H exchange is found to be covalent and olefin chemisorption is an intermediate case. Hence the sensitivity to the substitution for olefin chemisorption is expected to be less than other reactions (such as the methyl shift). To investigate these differences five examples of this reaction were considered: chemisorption of ethene, propene (in the primary and secondary positions), and of *i*-butene (in the primary and tertiary positions).

The olefin chemisorption reaction starts with the formation of a pi-complex, which converts via a ring-like transition state to an alkoxide. The calculated main geometry parameters and charges of the olefin chemisorption transition states are shown in Table 1 and illustrated in Fig. 1b where the atoms O1, C1, etc., are also labelled. In the transition states distances O1–C1 (1.993–2.449 Å), O2–H1 (1.202–1.405 Å), and C2–H1 (1.231–1.398 Å) are longer than normal O–C, O–H, and C–H bonds respectively, indicating rupture/formation of the bond. Distances C1–C2 (1.392–1.412 Å) are intermediate between single and double C–C bonds, indicating conversion of a double to single bond during the reaction. The calculated π-complex formation heats, activation energies (from the π-complex level) and chemisorption heats (from the free olefin level) are presented in Table 2 and Fig. 1c (the best estimates are the MP2/6-31G*//3-21G level values).

The reaction pathways, transition state geometries and activation energies for olefin

Table 1
The most important geometry parameters of the transition states of olefin chemisorption in the primary (p), secondary (s) and tertiary (t) positions

Reaction	Distances				Charges		
	O1–C1	O2–H1	C1–C2	C2–H1	q(C1)	q(C2)	q(H1)
Ethene (p)	1.993	1.202	1.395	1.398	+0.166	−0.686	+0.608
Propene (s)	2.151	1.280	1.399	1.320	+0.285	−0.641	+0.583
Propene (p)	2.042	1.250	1.392	1.345	+0.171	−0.535	+0.593
i-butene (t)	2.449	1.405	1.412	1.231	+0.405	−0.564	+0.510
i-butene (p)	2.080	1.289	1.392	1.311	+0.178	−0.380	+0.569

Distances in Ångstroms, charges in multiples of the electron charge.

chemisorption are found to be very similar to those reported in the previous quantum–chemical studies [3,7,25–27]. However, in this work the five different examples (Tables 1 and 2) are calculated with the same model cluster and the same theory level and therefore can be easily compared. Their comparison leads to the following conclusions.

Firstly, it can be seen that substitution of hydrogens attached to the C1 carbon atom (see Fig. 1b) by one or two methyl groups decreases the activation energy on average by 3.3 kcal/mol per methyl group (compare the ethene(p), propene(s), and *i*-butene(t) reactions). On the other hand, methyl substitutors on the C2 carbon atom increase the activation energy by 2.8 kcal/mol on average (compare the ethene(p), propene(p), and *i*-butene(p) reactions). This can be rationalised by the charge distribution in the transition states since the C1 carbon atom has a positive charge of +0.166–+0.405 eV (see Table 1) whereas the C2 carbon has a negative charge of −0.380–−0.686 eV.

Secondly, the differences in activation energies for the adsorption of a given olefin in different positions (6.5 and 12.1 kcal/mol for propene and *i*-butene respectively) are significantly greater than the differences in reaction heats (3.0 and 3.7 kcal/mol). This supports the suggestion [7] that at low temperatures the distribution of the olefin chemisorption products is not due to the different stability of tertiary, secondary and primary alkoxides but due to the different activation barriers for their formation. However, in view of the low activation energies involved, at higher temperatures all alkoxides are likely to be accessible and the (small) difference in alkoxide energy will give somewhat different equilibrium populations. This will not

Table 2
π-complex formation heats ΔH_π, activation energies $E^\#$ and reaction heats ΔH of olefin chemisorption reactions in the primary (p), secondary (s) and tertiary (t) positions

Reaction	ΔH_π		$E^\#$		ΔH	
	HF/3-21G	MP2/6-31G*//3-21G	HF/3-21G	MP2/6-31G*//3-21G	HF/3-21G	MP2/6-31G*//3-21G
Ethene (p)	−5.9	−7.5	36.9	30.7	−20.2	−24.5
Propene (s)	−6.6	−8.4	35.6	27.2	−20.3	−25.0
Propene (p)	−6.6	−8.4	41.2	33.7	−18.6	−22.0
i-butene (t)	−7.1	−9.0	35.4	24.2	−16.7	−23.0
i-butene (p)	−7.1	−9.0	44.8	36.3	−16.4	−19.3

Calculated at the HF/3-21G and the MP2/6-31G*//3-21G levels (kcal/mol).

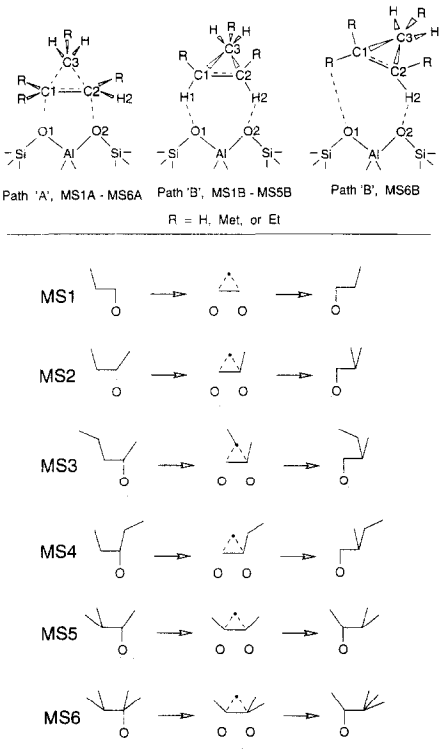

Fig. 2. Schemes of the alkyl shift transition states.

be the case for slower reactions such as a methyl shift.

3.2. Methyl shift

A methyl shift is the most obvious of several possible paths for the skeletal isomerisation of hydrocarbons. The hydrocarbons in zeolite catalysts are initially converted to surface alkoxides due to either the olefin chemisorption reaction or the hydride transfer reaction. The position of a methyl side group is then shifted along the alkoxide as is shown in Fig. 2. If this occurs at the end of the alkoxide or a larger alkyl group is transferred in the centre of the alkoxide, this results in a change in branching. There is experimental evidence that the activation energy is higher for isomerisation with branching than without branching [8,10]. This is important in the determination of the product distribution of this and other processes (e.g., alkylation). Other possible paths for the isomerisation are the dimerisation/cracking of the olefin and the closure/opening of the cyclopropane ring which will be discussed in a forthcoming paper [33].

The transition state geometry for the zeolite-catalysed methyl shift reaction has been found in the previous quantum–chemical calculations [7], but only two examples were considered in that work. Now we consider six examples of the methyl shift reaction calculated with the same model cluster and the same theory level. Comparison of these examples will allow an understanding of the influence of the substitutors at the reaction centre on the activation energies and to compare skeletal isomerisation of different hydrocarbons.

3.2.1. Geometries of the transition states

The calculated methyl shift transition states are sketched and the atoms involved in them are labelled in Fig. 2. Ball and stick pictures of the transition states for the methyl shift in 2,3-dimethylbut-2-oxide (reactions MS6A and MS6B) are given in Figs. 3 and 4. All the transition states contain a ring of three carbon atoms as was found in the previous calculations [7]. The C1–C3, C2–C3 bonds of the ring (1.640–2.237

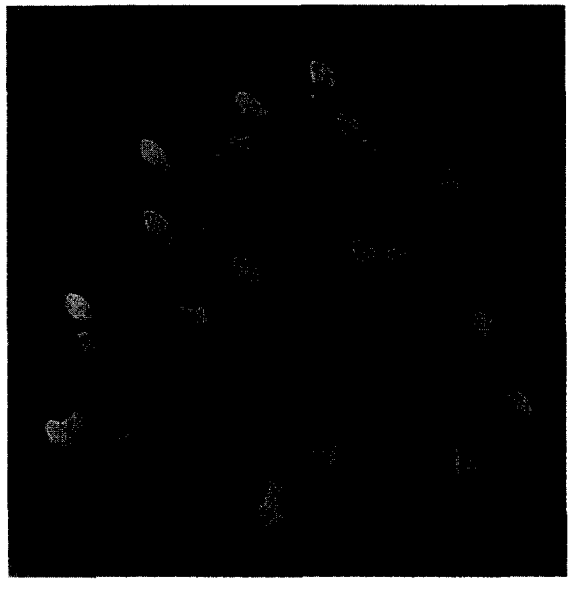

Fig. 3. Transition state for methyl shift in 2,3-dimethylbut-2-oxide, path 'A' (MS6A).

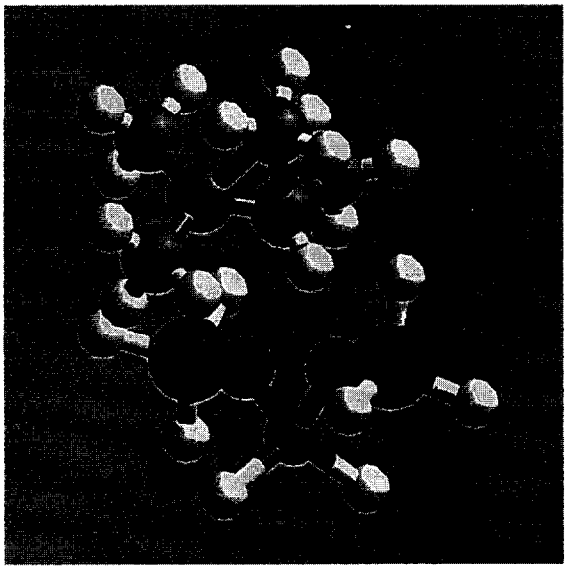

Fig. 4. Transition state for methyl shift in 2,3-dimethylbut-2-oxide, path 'B' (MS6B).

Å, see Table 3) are longer than a single C–C bond. This is because one bond is being ruptured and the other is being formed in the transition state. In contrast, the C1–C2 bond lengths in the ring (1.377–1.424 Å) are shorter than a single C–C bond.

The lifting of the symmetry constraints (imposed in the previous work [7]) gave a more complex potential energy surface and two transition states were found for each reaction. The difference between the two transition states lies in the orientation of the hydrocarbon fragment relative to the acid site. In the first set of transition states (labelled 'A'), the planes O1–Al–O2 and C1–C2–C3 are almost parallel; this is very similar to the results of the previous work [7]. In the second set (labelled 'B'), the planes O1–Al–O2 and C1–C2–C3 are almost perpendicular, and one or two hydrogen bonds are formed between the oxygen atoms of the site and hydrogen atoms bound to the C1 and C2 atoms of the hydrocarbon portion. This second pathway therefore involves reorientation of the hydrocarbon fragment during the reaction. For the majority of the reactions (MS1-4) the first pathway ('A') is found to be lower in energy (by 3–8 kcal/mol — see Table 4) but for MS5 and MS6 the second pathway ('B') is found to be easier (by 3–5 kcal/mol).

The most complicated potential energy profile was surprisingly found for the simplest reaction — a methyl shift in prop-1-oxide (MS1B). The HF/3-21G path for this reaction contains three saddle points separated by two high-energy minima. The symmetric transition state (MS1B in Table 3) is the highest point at the HF/3-21G level. However, the two asym-

Table 3
The most important geometry parameters of the transition states for methyl shift

Reaction	Distances							Charges		
	O1–C1	O1–H1	O2–C2	O2–H2	C1–C2	C1–C3	C2–C3	q(C1)	q(C2)	q(C3)
MS1A	2.426	2.423	2.426	2.423	1.383	1.921	1.921	+0.032	+0.032	−0.433
MS1B	2.876	1.909	2.876	1.909	1.377	1.899	1.899	−0.063	−0.063	−0.277
MS2A	2.683	2.326	2.471	2.448	1.382	1.919	1.904	+0.094	+0.021	−0.417
MS2B	3.119	2.445	2.707	1.610	1.424	1.640	2.237	−0.097	+0.168	−0.332
MS3A	2.705	2.369	2.477	2.447	1.378	1.927	1.927	+0.075	+0.014	−0.325
MS3B	3.183	2.347	2.761	1.682	1.405	1.703	2.138	−0.219	+0.159	−0.149
MS4A	2.708	2.339	2.472	2.443	1.383	1.914	1.902	+0.057	+0.030	−0.417
MS4B	3.141	2.288	2.715	1.624	1.421	1.648	2.207	−0.116	+0.164	−0.343
MS5A	2.769	2.562	2.886	2.523	1.383	1.897	1.924	+0.063	+0.087	−0.398
MS5B	2.925	1.934	2.925	1.934	1.385	1.899	1.899	+0.029	+0.029	−0.294
MS6A	3.222	—	2.727	2.366	1.390	1.892	1.924	+0.141	+0.104	−0.391
MS6B	3.140	—	2.904	1.835	1.391	1.945	1.868	+0.177	+0.041	−0.385

Distances in Ångstroms, charges in multiples of the electron charge.

metric saddle points (not shown in Table 3) were found to lie higher than the symmetric one at the MP2/6-31G*//3-21G level. Therefore the MP2/6-31G*//3-21G activation energy for the MS1B reaction given in Table 4 corresponds to these asymmetric transition states. Such a complex potential energy profile might be an artefact of the HF/3-21G level used for the geometry optimisation, but this subject was not investigated further since (i) the (degenerated) methyl shift in prop-1-oxide is less important than other reactions considered, and (ii) no complications were found in the lowest-energy path for this reaction (MS1A) and in both paths 'A' and 'B' for all other reactions (MS2-6).

The calculated reaction heats and activation energies are given in Table 4. Comparing these results to the previous calculation for the 3-methylbut-2-oxide [7] it can be seen that the effect of lifting the symmetry constraints decreases the calculated activation energy by 8.1 kcal/mol at the MP2/6-31G*//3-21G level. This is due to a relaxation of the hydrocarbon out of the plane of the cluster. The effect on the activation energies is limited but it is still much larger than the effect for the olefin chemisorption which was found to be less than 1.5 kcal/mol. This suggests that the large differences in activation energy between different reaction steps calculated in Ref. [7] with planar symmetry are likely to be confirmed by non-planar calculations but that details are not well predicted by planar calculations. The geometries of the transition states for pathway 'A' resemble the planar symmetric versions but no equivalent of the 'B' pathways are possible in the planar calculations (the hydrogens are constrained to lie out of the plane of the acid site).

3.2.2. Dependence of the activation energies on the methyl substitutors at the reaction centre

The examples were chosen to study the effect of the methyl substitutors in different positions on the activation energy of the methyl shift. The lowest energy path ('A' or 'B' — see previous section) for each reaction will be considered.

From Table 4 it can again be seen that the reaction heats of methyl shift are small (less than 3 kcal/mol) and do not differ greatly between reactions (due to the lack of a significant energy ordering of the alkoxide species). There is therefore again little driving force for any of the reactions and the relative ease of the reaction steps is governed by the activation energies — i.e. the stabilisation of the transition states by substitution will determine the relative rates of the isomerisation of different alkoxides.

The addition of methyls to either the C1 or

Table 4
Reaction heats ΔH and activation energies $E^{\#}$ of methyl shift reactions, calculated at the HF/3-21G and the MP2/6-31G*//3-21G levels (kcal/mol)

Reaction	ΔH		$E^{\#}$, Path 'A'		$E^{\#}$, Path 'B'	
	HF /3-21G	MP2 /6-31G*//3-21G	HF /3-21G	MP2 /6-31G*//3-21G	HF /3-21G	MP2 /6-31G*//3-21G
MS1: propane → propane	0	0	81.3	*65.9*	73.5	70.2
MS2: *n*-butane → *i*-butane	+0.8	+2.6	76.1	*61.6*	71.0	69.5
MS3: *n*-pentane → *i*-pentane (via ethyl shift)	+0.3	+2.5	75.6	*60.6*	70.1	63.1
MS4: *n*-pentane → *i*-pentane	−0.2	+2.5	75.8	*60.9*	71.5	69.1
MS5: *i*-pentane → *i*-pentane (shift of the existing branch)	0	0	69.1	54.0	63.6	*50.9*
MS6: 2,3-dimethylbutane → 2,2-dimethylbutane	+1.4	+1.6	66.0	50.7	58.8	*46.3*

In italics: best estimations of the activation energies.

C2 carbon atoms (see Fig. 2) significantly decreases the activation energy as can be seen from Table 4. Comparison of the activation energies for the prop-1-oxide, but-2-oxide, 3-methylbut-2-oxide and 2,3-dimethylbut-2-oxide (reactions MS1, MS2, MS5 and MS6, respectively) shows that the activation energy is decreased by an average of 5.7 kcal/mol for each additional methyl group on the C1 and C2 carbons. This may be expected from the charges found on these two atoms in the transition state (see Table 3). This stabilisation has a large impact on the relative rates of the reactions in the different compounds but it is much less than the stabilisation observed for free carbenium ions (the energy difference between free ethyl and s-propyl cations reported in Ref. [34] is 19 kcal/mol for instance). This shows that there is significant stabilisation of the positively charged hydrocarbon portion by the zeolite surface in the transition state.

In addition to the methyl shift the shift of larger alkyl groups has been investigated. Such reactions were considered in Ref. [10] and possibly occur during isomerisation. This is an analogue of the methyl shift with substitution at the C3 carbon atom. It can be seen from Table 4 that the effect of this substitution is small in comparison to the substitution on the C1 and C2 atoms. The difference between the calculated activation energies for the methyl shift in but-2-oxide and the ethyl shift in pent-3-oxide (MS2 and MS3) is only 1.0 kcal/mol. This difference can also be rationalised by the large negative charge seen on C3 (see Table 3).

Finally, the effect of methyl group substitution outside the ring-like structure in the transition state is small as can be seen from the small activation energy difference calculated between methyl shifts in but-2-oxide and pent-2-oxide (MS2 and MS4). This suggests that the substitution at the reactive centre has a significant effect on the reaction rate but substitution away from this centre has little effect. This supports the use of smaller molecules as models for the reactions of larger hydrocarbons.

3.2.3. Comparison of different types of skeletal isomerisation

As mentioned above the methyl shift reaction is one of the possible mechanisms for skeletal isomerisation. The reactions investigated allow the comparison of different classes of isomerisations and the qualitative comparison of the calculated results to experiment.

Firstly, isomerisation involving a change in the branching of a linear alkoxide (reactions MS2 and MS3) can be compared with the shift in the position of a side group without change in the branching of the alkoxide such as the methyl shift in 3-methylbut-2-oxide (MS5). The change in branching is predicted to be about 10 kcal/mol harder in qualitative agreement with a row of the experimental rate constants [8]. It can also be seen that neighbouring branches facilitate the shift of a side group — the activation energy for the methyl shift in 2,3-dimethylbut-2-oxide (reaction MS6) is a further 4.5 kcal/mol lower.

Secondly, these results suggest that the ethyl shift (and by extension shifts of larger alkyl groups) are possible as well as the methyl shift. This follows from the comparison of the methyl shift in but-2-oxide (MS2) and ethyl shift in pent-3-oxide (MS3) which have activation energies within 1 kcal/mol of each other. Such reactions represent an interesting possibility for isomerisation mechanisms especially in wide-pore zeolites where the shift of a larger alkyl group would not be sterically hindered.

Finally the calculated activation energies suggest that the methyl shift in *n*-butyl alkoxide to form an isobutyl alkoxide (reaction MS2) has a similar activation energy to the isomerisation of larger *n*-alkoxides (e.g., *n*-pentoxide isomerisation, reaction MS3 and MS4). Hence if this was the mechanism for the isomerisation, little difference would be predicted for the rates of the isomerisation of the *n*-butane and *n*-pentane. However, a significant difference is found experimentally [8,11,12]. The difference in skeletal isomerisation of *n*-butane and larger *n*-alkanes can be rationalised by the cyclopropane

ring path [35,36]. Calculations on this mechanism will be discussed in a forthcoming paper [33].

3.3. Influence of the zeolite acid strength on the activation energies of the olefin chemisorption and methyl shift reactions

One of the parameters that distinguish different catalysts is the strength of their acid sites which appears to influence both the activity and product selectivities for different processes. This effect can be investigated in quantum chemical calculations by constraining the lengths of the terminal Si–H bonds of the cluster [5,6,37]. The influence of the acid strength on the activation energies for many of the catalytically important reaction steps has been investigated in Ref. [7] where a correlation was found between the degree of ionicity of the transition state and the sensitivity to the acidity. However, these results are for the HF/3-21G level of calculation and with symmetry constraints and do not show whether methyl substitution has an effect on the sensitivity to acid strength. These calculations have been extended for ethene chemisorption and methyl shift in 3-methylbut-2-oxide at the MP2/6-31G*//3-21G level and without symmetry constraints. It is also interesting to see if the influence of the acid strength matches with the influence of the methyl substitution seen in the previous section, as would be expected if the system is driven solely by the ionicity of the transition state.

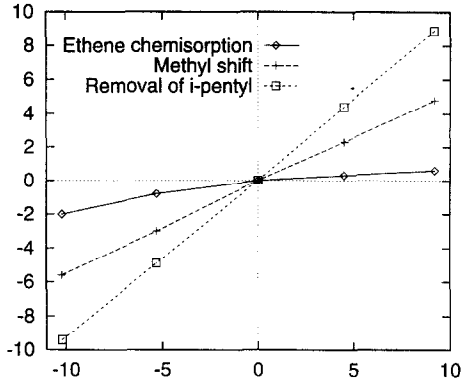

Fig. 5. Variations of the activation energies for ethene chemisorption and methyl shift in 2-methylbut-2-oxide and of the *i*-pentyl removal energy (kcal/mol, vertical axe) on the acid site deprotonation energy (kcal/mol, horizontal axe).

In the calculations five acid site clusters were used. Four had the lengths of the terminal Si–H bonds of the cluster and were set at 1.300, 1.400, 1.600, and 1.700. The fifth was the optimised cluster where the Si–H distance are close to 1.5 (from 1.47–1.50). The calculated activation energies are shown in Table 5 and Fig. 5 together with deprotonation energies of the model acid sites. These variations in the activation energies can be related to measured infrared shifts on the adsorption of a weakly coordinating base such as carbon monoxide [38] or the ammonia chemisorption energy.

The results suggest that the activation energy for the methyl shift decreases strongly with

Table 5
Activation energies (kcal/mol) for ethene chemisorption and methyl shift in 3-methylbuto-2-xide

	Cluster				
	cluster 1	cluster 2	cluster 3	cluster 4	cluster 5
Si–H distances, in the cluster (Å):	1.300	1.400	optimized (1.47–1.50)	1.600	1.700
Parameter					
ΔH_{depr}	319.2	314.5	310.0	304.7	299.8
ΔH_{π}	−7.0	−7.3	−7.5	−7.9	−7.6
$E^{\#}_{chemisorption}$	31.3	31.0	30.7	29.9	28.7
$E^{\#}_{methyl\ shift}$	55.7	53.2	50.9	47.9	45.3
$\Delta H_{remove\ i\text{-}pentyl}$	142.2	137.7	133.3	128.4	123.9

Calculated at the MP2/6-31G*//3-21G level with the clusters of different acid strength.

increasing acid strength (decreasing by 10.4 kcal/mol for a variation of the site deprotonation energy of 19.4 kcal/mol). In contrast, the activation energy for the ethene chemisorption has a much weaker dependence on the acid strength. The activation energy (relative to the π-complex level) changes only by 2.6 kcal/mol for a change in the deprotonation energy of 19 kcal/mol.

This difference in the response to the acid strength can be rationalised by the charges present. The methyl shift transition state is essentially ionic with the alkoxide bonds being largely broken. Changes in the acid strength therefore give a strong stabilisation of the transition state. In contrast, the olefin chemisorption transition state is partially covalent since the hydrogen atom transferring still interacts with the surface oxygen (see Fig. 1b and Table 1) and the effect of acid strength is reduced. This supports the conclusions of the previous works [5–7] which found three broad classes of acid-catalysed reactions in zeolites: covalent (D/H exchange), intermediate (olefin chemisorption) and ionic (many other reactions, e.g., methyl shift and β-scission).

It can be seen that the acid strength variations have little effect on the olefin chemisorption compared to the methyl shift whereas the influence of methyl substitution is stronger.

Finally, it can be seen that the difference in the effect of the acid strength is somewhat stronger than in the effect of the substitution by methyl groups discussed in the previous section (where the activation energy differences on substitution at the C1 atom were only a factor 2 different). This suggests that the broad influence of the acidity and the methyl substitution can be rationalised by considering the charges but the details are more complex since the zeolite still has a stabilising effect on the activation energy. Such stabilisation follows from a consideration of the variation with acid strength of the energy of an infinitely separated deprotonated site and a carbenium ion (shown in Table 5). This energy varies by 18.3 kcal/mol, compared to the 10.6 kcal/mol variation in the methyl shift activation energy. Hence even for this ionic reaction, the hydrocarbon portion of the transition state is not completely similar to a free carbocation.

3.4. Absolute values of the activation energies

The previous sections of this paper focused on the activation energy changes with change of the hydrocarbon or variation of the zeolite acid strength. The differences in activation energies are of great interest as they determine the product distribution of the reactions, and such differences are expected to be well predicted by the present calculations due to cancellation of errors. However, it can be shown that the calculated absolute values of the activation energies are systematically overestimated. There are three reasons for this. Firstly, the acid strength of the model cluster used in the calculations (Cluster 3 in Table 5, deprotonation energy 310.0 kcal/mol) is lower than that of typical zeolite acid sites (deprotonation energy — about 295 kcal/mol according to Ref. [39]). This would account for around 8 kcal/mol of the difference in activation energy for the methyl shift (but only around 2 kcal/mol for olefin chemisorption), using the variations of these energies with acid strength described in the previous section. Secondly, our cluster model does not take into account interactions between the positive hydrocarbon portion of the transition state and the oxygen atoms in other portions of the zeolite cage. Such interaction should stabilise the transition state [40]. Finally, the moderate size of the basis set used (6-31G*) and approximate character of the correlation corrections due to the MP2 theory could contribute to the overestimation.

The calculated activation energies for olefin chemisorption (30.7 kcal/mol for ethene (p) and 27.2 kcal/mol for propene (s), see Table 2) are to be compared with the experimental values for ethene (true activation energy on HY zeolite is 25–28 kcal/mol [41]) and propene (estimated

true activation energy is 21 kcal/mol [42]). The comparison shows that the activation energies for olefin chemisorption given in Table 2 are overestimated by about 5 kcal/mol.

The activation energies for methyl shift should be affected stronger than those for olefin chemisorption as the former reaction is ionic and the latter is semi-covalent [7]. Experimental measurement of the methyl shift activation energy is difficult but the correction for the activation energy can be found indirectly. For this we used another zeolite-catalysed reaction, the monomolecular (protolytic) cracking of alkanes. This reaction can be studied in isolation (secondary reactions are of minor importance when conversion of an alkane is low) and has an ionic transition state [7], hence errors in the calculated activation energies for protolytic cracking and for methyl shifts are expected to be similar. The experimental activation energies for protolytic cracking (47.3 kcal/mol for propane cracking on HZSM-5 [43] and 39.6–40.6 kcal/mol for *i*-butane cracking on USY-1 and USY-2 [44]) are to be compared with the calculated values (67.6 kcal/mol for propane and 59.9 kcal/mol for *i*-butane cracking, the theoretical model being the same as that for the methyl shift). Comparison of these data indicates that the activation energies for an ionic reaction are overestimated by about 20 kcal/mol in our calculations. This figure should be substracted from the methyl shift activation energies given in Table 4.

4. Conclusion

Quantum–chemical calculations of the olefin chemisorption and methyl shift reactions have been carried out. Differences between hydrocarbons and effects of the acid strength of the site and the symmetry constraints imposed on previous calculations were investigated. The conclusions can be summarised as follows:

(1) Products of the reactions. The product distribution of the methyl shift reaction is determined by the activation energy rather than the difference in stability of the reactants and products. The variation in activation energy will also be significant for the product distribution of olefin chemisorption at low temperatures, but at higher temperatures the alkoxides will come into thermal equilibrium.

(2) Influence of additional methyl groups on the activation energies. In both reactions there are electropositive carbon atoms in the transition state (two for the methyl shift and one for the olefin chemisorption). Methyl substitutions on these atoms significantly decrease the calculated activation energies (on average by 6.5 kcal/mol per group in methyl shift and 3.3 kcal/mol in olefin chemisorption). This mirrors and rationalises the reactivity ordering deduced from the carbenium ion model even though the reaction intermediates are not carbenium ions. Substitution on other carbon atoms has little or no effect.

(3) The effect of acid strength changes. The effect of the acid strength of the site involved shows more differences between the two reactions. A variation of 19 kcal/mol in the site deprotonation energy gives a change in activation energy of 10.4 kcal/mol for the methyl shift and only 2.6 kcal/mol for the olefin chemisorption. This shows that the effect of the methyl substitution and acid strength variation are not the same.

(4) Skeletal isomerisation with and without change of branching. Branch formation in linear alkanes is found to be about 10 kcal/mol more difficult than the shift of an existing branch, in quantitative agreement with the experimental data. A second neighbouring branch further facilitates the shift.

(5) Skeletal isomerisation of *n*-butane and *n*-pentane. It is likely that at least one of these reactions does not proceed via this one-step process, since only a small difference in activation energy is predicted in contrast to the experimental observation of large differences. The reaction (at least for *n*-pentane) is thought to

proceed through another mechanism (e.g., cyclopropane or dimerisation/cracking).

(6) Shifts of other alkyl groups. The calculations show that a shift of ethyl and larger alkyl groups is possible, especially in wide-pore zeolites. This implies that this reaction mechanisms not usually considered may be involved in zeolite catalysed reactions.

(7) Symmetry constraints. The transition states obtained with symmetry constraints are found to be qualitatively correct but the absolute activation energies calculated may be overestimated by up to 8–10 kcal/mol. The effect on relative activation energies is expected to be small.

References

[1] B.C. Gates, Catalytic Chemistry, John Wiley and Sons, New York, 1992.
[2] I.E. Maxwell, W.H.J. Stork, in: H. van Bekkum, E.M. Flanigen, J.C. Jansen (Eds.), Introduction to Zeolite Science and Practice, Elsevier, Amsterdam, 1991, p. 571.
[3] I.N. Senchenya, V.B. Kazansky, Catal. Lett. 8 (1991) 317.
[4] V.B. Kazansky, Acc. Chem. Res. 24 (1991) 379.
[5] G.J. Kramer, R.A. van Santen, C.A. Emeis, A.K. Nowak, Nature 363 (1993) 529.
[6] G.J. Kramer, R.A. van Santen, J. Am. Chem. Soc. 117 (1995) 1766.
[7] A.M. Rigby, G.J. Kramer, R.A. van Santen, J. Catal. 170 (1997) 1–10.
[8] F. Chevalier, M. Guisnet, R. Maurel, in: G.C. Bond, P.B. Wells, F.C. Tompkins (Eds.), Proceedings of the 6th International Congress on Catalysis, The Chemical Society, London, 1977, p. 478.
[9] J. Weitkamp, Ind. Eng. Chem. Prod. Res. Dev. 21 (1982) 550.
[10] J.A. Martens, P.A. Jacobs, in: J.B. Moffat (Ed.), Theoretical Aspects of Heterogeneous Catalysis, Van Nostrand Reinhold, New York, 1990, p. 52.
[11] G. Zi, C. Jian-min, H. Wei-ming, T. Yi, Stud. Surf. Sci. Catal. (Acid-Base Catalysis II) 90 (1994) 507.
[12] H. Liu, G.D. Lei, W.M.H. Sachtler, Appl. Catal. A 137 (1996) 167.
[13] C. Bearez, F. chevalier, M. Guisnet, React. Kinet. Catal. Lett. 22 (1983) 405.
[14] N.N. Krupina, A.L. Proskurnin, A.Z. Dorogochinskii, React. Kinet. Catal. Lett. 32 (1986) 135.
[15] J.A. Maness, K.M. Dooley, J. Catal. 117 (1989) 322.
[16] A. Corma, M.I. Juan-Rajadell, J.M. Lopez-Nieto, A. Martinez, C. Martinez, Appl. Catal. A 111 (1994) 175.
[17] R.A. Asuquo, G. Eder-Mirth, J.A. Lercher, J. Catal. 155 (1995) 376.
[18] K.-J. Chao, H.-C. Wu, L.-J. Leu, J. Catal. 157 (1995) 289.
[19] M. Guisnet, P. Andy, N.S. Gnep, E. Benazzi, C. Travers, J. Catal. 158 (1996) 551.
[20] M.A. Asensi, A. Corma, A. Martinez, J. Catal. 158 (1996) 561.
[21] F. Garin, L. Seyfried, P. Girard, G. Maire, A. Abdulsamad, J. Sommer, J. Catal. 151 (1995) 26.
[22] W.-Q. Xu, Y.-G. Yin, S.L. Suib, J.C. Edwards, C.-L. O'Young, J. Phys. Chem. 99 (1995) 9443.
[23] H.C. Woo, K.H. Lee, J.S. Lee, Appl. Catal. A 134 (1996) 147.
[24] A. Corma, A. Martinez, C. Martinez, Appl. Catal. A 134 (1996) 169.
[25] P. Viruela-Martin, C.M. Zicovich-Wilson, A. Corma, J. Phys. Chem. 97 (1993) 13713.
[26] E.M. Evleth, E. Kassab, H. Jessri, M. Allavena, L. Montero, L.R. Sierra, J. Phys. Chem. 100 (1996) 11368.
[27] V.B. Kazansky, M.V. Frash, R.A. van Santen, Appl. Catal. A 146 (1996) 225.
[28] M.F. Guest, P. Fantuicci, R.J. Harrison, J. Kendrick, J.H. van Lenthe, K. Schoeffel, P. Sherwood: GAMESS-UK User's Guide and Reference Manual 1: Revision C.0, Computing for Science (CFS) Ltd., Daresbury Laboratory, Daresbury, 1993.
[29] W.J. Hehre, L. Radom, P.v.R. Schleyer, J.A. Pople, Ab Initio Molecular Orbital Theory, John Wiley and Sons, New York, NY, 1986.
[30] M.S. Gordon, Chem. Phys. Lett. 76 (1980) 163.
[31] M.M. Francl, W.J. Pietro, W.J. Hehre, J.S. Binkley, M.S. Gordon, D.J. DeFrees, J.A. Pople, J. Chem. Phys. 77 (1982) 3654.
[32] A.J. Stone, Chem. Phys. Lett. 83 (1981) 233.
[33] A.M. Rigby, M.V. Frash, in preparation.
[34] F.P. Lossing, J.L. Holmes, J. Am. Chem. Soc. 106 (1984) 6917.
[35] D.M. Brouwer, J.M. Oelderik, Rec. Trav. Chim. 87 (1968) 721.
[36] D.M. Brouwer, H. Hogeveen, Progr. Phys. Org. Chem. 9 (1972) 179.
[37] S.R. Blaszkowski, M.A.C. Nascimento, R.A. van Santen, J. Phys. Chem. 100 (1996) 3463.
[38] M.V. Frash, M.A. Makarova, A.M. Rigby, J. Phys. Chem. B 101 (1997) 2116.
[39] H.V. Brandt, L.A. Curtiss, L.E. Iton, J. Phys. Chem. 97 (1993) 12773.
[40] S. Ramachandran, T.G. Lenz, W.M. Skiff, A.K. Rappe, J. Phys. Chem. 100 (1996) 5898.
[41] N.W. Cant, W.K. Hall, J. Catal. 25 (1972) 161.
[42] J. Engelhardt, W.K. Hall, J. Catal. 125 (1990) 472.
[43] T.F. Narbeshuber, H. Vinek, J.A. Lercher, J. Catal. 157 (1995) 388.
[44] A. Corma, P.J. Miguel, A.V. Orchilles, J. Catal. 145 (1994) 171.